

# Direct Regulation of Cytochrome *c* Oxidase by Calcium Ions

Tatiana Vygodina, Anna Kirichenko, Alexander A. Konstantinov\*

A. N. Belozersky Institute of Physico-Chemical Biology, M. V. Lomonosov Moscow State University, Moscow, Russia

## Abstract

Cytochrome *c* oxidase from bovine heart binds  $\text{Ca}^{2+}$  reversibly at a specific Cation Binding Site located near the outer face of the mitochondrial membrane.  $\text{Ca}^{2+}$  shifts the absorption spectrum of heme *a*, which allowed previously to determine the kinetics and equilibrium characteristics of the binding. However, no effect of  $\text{Ca}^{2+}$  on the functional characteristics of cytochrome oxidase was revealed earlier. Here we report that  $\text{Ca}^{2+}$  inhibits cytochrome oxidase activity of isolated bovine heart enzyme by 50–60% with  $K_i$  of  $\sim 1 \mu\text{M}$ , close to  $K_d$  of calcium binding with the oxidase determined spectrophotometrically. The inhibition is observed only at low, but physiologically relevant, turnover rates of the enzyme ( $\sim 10 \text{ s}^{-1}$  or less). No inhibitory effect of  $\text{Ca}^{2+}$  is observed under conventional conditions of cytochrome *c* oxidase activity assays (turnover number  $>100 \text{ s}^{-1}$  at pH 8), which may explain why the effect was not noticed earlier. The inhibition is specific for  $\text{Ca}^{2+}$  and is reversed by EGTA.  $\text{Na}^+$  ions that compete with  $\text{Ca}^{2+}$  for binding with the Cation Binding Site, do not affect significantly activity of the enzyme but counteract the inhibitory effect of  $\text{Ca}^{2+}$ . The  $\text{Ca}^{2+}$ -induced inhibition of cytochrome *c* oxidase is observed also with the uncoupled mitochondria from several rat tissues. At the same time, calcium ions do not inhibit activity of the homologous bacterial cytochrome oxidases. Possible mechanisms of the inhibition are discussed as well as potential physiological role of  $\text{Ca}^{2+}$  binding with cytochrome oxidase.  $\text{Ca}^{2+}$ -binding at the Cation Binding Site is proposed to inhibit proton-transfer through the exit part of the proton conducting pathway H in the mammalian oxidases.

**Citation:** Vygodina T, Kirichenko A, Konstantinov AA (2013) Direct Regulation of Cytochrome *c* Oxidase by Calcium Ions. PLoS ONE 8(9): e74436. doi:10.1371/journal.pone.0074436

**Editor:** Oleg Y. Dmitriev, University of Saskatchewan, Canada

**Received:** May 3, 2013; **Accepted:** August 1, 2013; **Published:** September 10, 2013

**Copyright:** © 2013 Vygodina et al. This is an open-access article distributed under the terms of the Creative Commons Attribution License, which permits unrestricted use, distribution, and reproduction in any medium, provided the original author and source are credited.

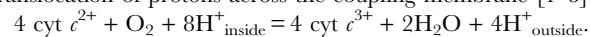
**Funding:** The work has been supported in part by Howard Hughes Medical Institute International Scholar Award 55005615 and Russian Fund for Basic Research grant 11-04-01330-a to AAK. The funders had no role in study design, data collection and analysis, decision to publish, or preparation of the manuscript.

**Competing Interests:** The authors have declared that no competing interests exist.

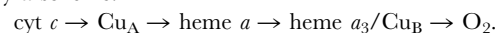
\* E-mail: konst@genebee.msu.su

## Introduction

Cytochrome *c* oxidase (COX) is a terminal enzyme of the mitochondrial and bacterial respiratory chains. The enzyme catalyses reduction of molecular oxygen to water coupled to translocation of protons across the coupling membrane [1–3]:



The electron transfer in the oxidase is mediated by four metal redox centers: two A-type hemes, low-spin *a* and high-spin *a*<sub>3</sub>, and two copper centers, a binuclear  $\text{Cu}_A$  and a mononuclear  $\text{Cu}_B$ . The high-spin heme *a*<sub>3</sub> iron and  $\text{Cu}_B$  are located within  $\sim 5 \text{ \AA}$  from each other and form a di-nuclear site of oxygen reduction to water. The sequence of electron transfer through the enzyme is described by a scheme.



In addition to the redox centers, cytochrome oxidases from mitochondria and many bacteria contain non-redox metal ions, revealed by chemical analysis [4] and identified later on in the crystal structure of the enzyme [5,6]. First, there is  $\text{Mg}^{2+}$  (or  $\text{Mn}^{2+}$ ) ion which holds together subunits I and II and may be part of the exit pathway for the pumped protons and for water formed in the active site [7–9]. Second, there is a zinc finger in subunit Vb of bovine heart oxidase [5,6], function of which is not known yet. Third, a novel metal cation binding site (CBS) was resolved in the 3D structure of COX from both mitochondria and bacteria (refs. [10,11] and PDB entry 1M56) that can harbour  $\text{Ca}^{2+}$  or  $\text{Na}^+$  ion.

Reversible binding of  $\text{Ca}^{2+}$  with the mitochondrial COX was described originally by Wikstrom and Saari [12], who reported a blue shift of the reduced heme *a*  $\alpha$ -absorption band induced by EDTA and showed that the effect was due to reversal of a red shift induced by adventitious calcium ions acting from the outer side of the mitochondrial membrane. The specific CBS was identified later on in the crystal structures of the A1-class [13] cytochrome oxidases from two bacteria (*P. denitrificans* [10] and *R. sphaeroides* (PDB entry 1M56)) and bovine heart [11].

As shown in **Figure 1A**, the site is located at the very periphery of subunit I facing the outer side of the membrane, within ca. 18 Å from the Fe ion of heme *a*. In the bacterial oxidases, the X-ray structure and chemical analysis reveal tightly bound  $\text{Ca}^{2+}$  at the site [14,15]. The cation cannot be removed by calcium chelators. Accordingly, addition of  $\text{Ca}^{2+}$  does not induce spectral shift of heme *a* in COX from *R. sphaeroides* [16] or *P. denitrificans* [14]. However, mutations in some of the residues in coordination sphere of  $\text{Ca}^{2+}$  in COX from *P. denitrificans* [14,17,18] or *R. sphaeroides* [15] result in release of the tightly bound cation and in reversible binding of  $\text{Ca}^{2+}$  with the bacterial enzyme, making the bacterial oxidases a useful model for the studies of CBS in the mammalian oxidase.

Originally reported to be absolutely specific for  $\text{Ca}^{2+}$  and proton [19], the CBS was shown later on to bind also  $\text{Na}^+$  as revealed by competition of the latter with  $\text{Ca}^{2+}$  [16,20]. Furthermore, the

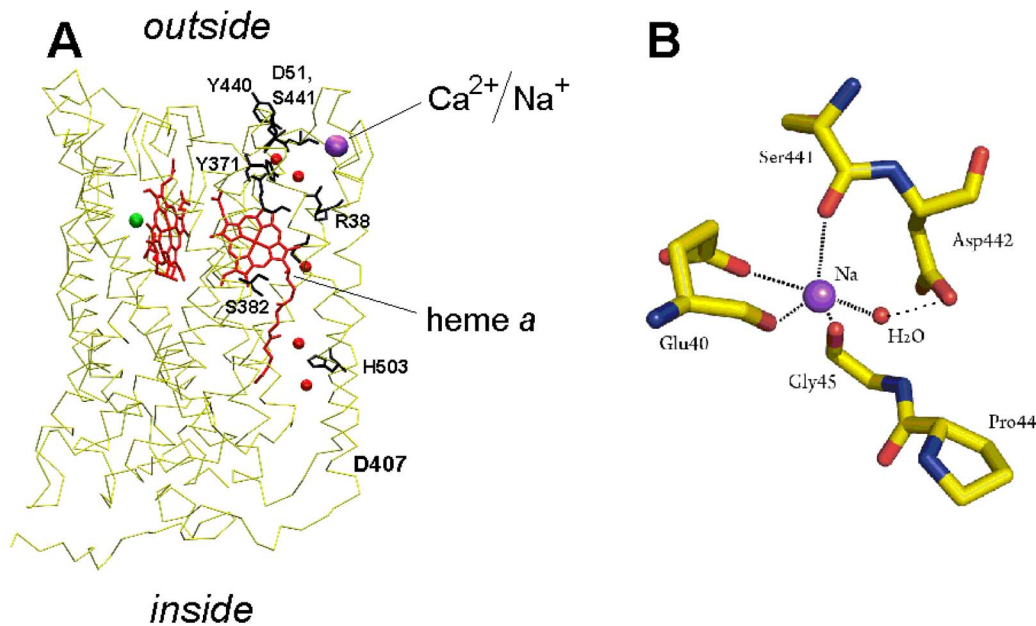


**Figure 1. The Cation Binding Site in cytochrome c oxidase.** (A) Location of the Cation Binding Site in subunit I of bovine enzyme and its relation to the proposed proton conducting pathway H. Components of the H-pathway are depicted as orange spheres (fixed water molecules) and black sticks (amino acid residues, A-propionate and carbonyl groups of heme *a*). Enlarged picture of the exit part of the H-channel is shown in Figure 8. (B) Coordination sphere of the bound cation in bovine oxidase. Based on the PDB 1V55 structure. doi:10.1371/journal.pone.0074436.g001

published crystal structure of the mitochondrial enzyme resolved  $\text{Na}^{+}$  rather than  $\text{Ca}^{2+}$  bound at the site (Figure 1B, ref. [11]). This is not surprising since the crystals were obtained at  $\sim 10$  mM  $\text{Na}^{+}$  in the buffer, that is well above  $K_d$  for  $\text{Na}^{+}$  binding with the site (ca.  $10^{-3}$  M [16]). Very recently, competing binding of  $\text{Ca}^{2+}$  and  $\text{Na}^{+}$  with CBS of bovine COX was confirmed by FTIR spectroscopy [21].

As  $\text{Ca}^{2+}$  brings about a red shift of heme *a* absorption spectrum in both the reduced and oxidized forms, it is easy to monitor binding of the cation with the enzyme at different oxidation states. Equilibrium and kinetic parameters of the binding have been studied in considerable detail for the mitochondrial and mutant bacterial oxidases [14–20]. Initially,  $K_d$  for  $\text{Ca}^{2+}$  binding with the mitochondrial oxidase was reported to be 20–30  $\mu\text{M}$  [12,19]. The values were so much higher than typical concentrations of free  $\text{Ca}^{2+}$  in the cytoplasm ( $\sim 10^{-7}$  M [22,23]) that calcium binding with COX was not considered to be of physiological relevance and did not receive much attention. However, subsequent studies with the use of  $\text{Ca}^{2+}$ -buffering systems determined much lower  $K_d$  value of  $\sim 1$   $\mu\text{M}$  [16,18], which is well in the range of cytoplasmic  $\text{Ca}^{2+}$  concentrations attained during the  $\text{Ca}^{2+}$  spikes induced by  $\text{Ca}^{2+}$  efflux from the cisterns of endoplasmic reticulum [22,23].

$\text{Ca}^{2+}$  is a ubiquitous intracellular signal transduction messenger that regulates a vast number of processes in the cell [22,23]. In particular,  $\text{Ca}^{2+}$  is known to enhance oxidative phosphorylation in mitochondria (reviewed, [24,25]) by stimulating activity of several Krebs cycle dehydrogenases in the mitochondrial matrix and also by activating several mitochondrial substrate transporters [26,27]. High affinity binding of  $\text{Ca}^{2+}$  with COX at a specific site at the outer face of the inner mitochondrial membrane implied that cytoplasmic  $\text{Ca}^{2+}$  could be a physiological effector of the mitochondrial COX [15,16,18]. Disappointingly, previous attempts to reveal any effect of  $\text{Ca}^{2+}$  on the functional characteristics of COX were not successful. In this paper, we describe inhibition of COX induced by  $\text{Ca}^{2+}$  binding at the CBS. The reasons why

this effect was not noticed earlier as well as possible mechanisms and physiological role of the  $\text{Ca}^{2+}$ -induced inhibition are discussed. The data were presented at the 2010 EBEC Meeting at Warsaw [28,29].

## Materials and Methods

### Chemicals

Sodium dithionite,  $\text{CaCl}_2$ , choline chloride (C-1879, >99%), carbonyl cyanide *m*-chlorophenyl hydrazone (CCCP), cyclosporine A, nagarse, cytochrome *c* type III,  $N,N,N',N'$ -tetramethyl-*p*-phenylenediamine (TMPD), potassium salts of ferrocyanide and ferricyanide, and calcium buffers: ethylene-bis(oxyethylenetriolo)-tetraacetic acid (EGTA), nitrilotriacetic acid (NTA), 1,2-bis(2-aminophenoxy)-ethane- $N,N,N',N'$ -tetraacetic acid (BAPTA) and  $N$ -(2-hydroxyethyl)ethylenediamine- $N,N,N',N'$ -triacetic acid (HEDTA) were from Sigma-Aldrich. pH buffers, sodium chloride and magnesium sulfate were purchased from Amresco. Dodecyl-maltoside (DM) “SOL-GRADE” was from Anatrace.

### Preparations

“Fast” COX was purified from bovine heart mitochondria using a modified protocol by Fowler et al. [30]. Bovine hearts were purchased from slaughterhouse “OOO Pushkinsky Meet House” (23 Sokolovstskaya str., Pushkino, Moscow region). The hearts were sold in agreement with the A.N.Belozersky Institute request letter under the condition that they may not be used for commercial purposes, but for scientific research purposes only. COX from *R. sphaeroides* was purified from bacterial membranes (a kind gift from Dr. R. Gennis laboratory at UIUC, IL) on a column with  $\text{Ni}^{2+}$ -NTA Sepharose (Qjagen) [31]. A sample of D477A mutant COX from *P.denitrificans* was kindly provided by Dr. Anne Puustinen (Helsinki Bioenergetics Group, University of Helsinki). Concentration of COX was determined from the “dithionite-reduced minus oxidized” difference absorption spectra using  $\Delta\epsilon_{605-630}$  of

27 mM<sup>-1</sup>cm<sup>-1</sup>. Mitochondria from rat tissues were isolated from outbred white male rats by conventional methods as used in this laboratory [32,33] with additional protease treatment (Nagarse) [34] to disrupt the outer mitochondrial membrane and remove permeability barrier for added cytochrome *c* and calcium ions. After the treatment, mitochondria were washed thoroughly to remove Nagarse. Animal protocols were approved by the Institutional Review Board. Handling of the animals and experimental procedures were conducted in accordance with the international guidelines for animal care and use and were approved by the Institutional Ethics Committee of A.N. Belozersky Institute of Physico-Chemical Biology at Moscow State University.

## Assays

Experiments with the isolated COX were performed in a basic medium containing 50 mM Tris/MES pH 8.0–8.2, 0.05% dodecyl maltoside, choline chloride (50 mM or higher as indicated), and also 100 μM EGTA to bind adventitious calcium and strip off the bound calcium from the mitochondrial oxidase. In order to slow down reaction of cytochrome *c* with COX, in some experiments we had to increase the ionic strength of the reaction mixtures. To this end, choline chloride was chosen as the main salt component of the reaction buffers because, in our experience, this salt as available from Sigma-Aldrich (C-1879) proved to have very low contamination with Na<sup>+</sup>. Concentration of sodium ions in the media has to be minimized because Na<sup>+</sup> competes with Ca<sup>2+</sup> for binding with COX [16,20]. In experiments with mitochondria, the basic buffer contained 0.25 M sucrose, 0.4 M choline chloride, 50 mM Tris/MES or Tris/HEPES pH 8, 100 μM EGTA and also 1 μM cyclosporine A and 1 μM the uncoupler, CCCP. Concentration of free calcium in the buffers at given concentrations of the added CaCl<sub>2</sub>, Ca<sup>2+</sup>-buffering chelators (EGTA, HEDTA, BAPTA, NTA) and other specific conditions was calculated as earlier [18] with a free software “WinMAXC, v.2.05”.

Spectrophotometric measurements were made in a Varian Cary300Bio or an SLM-Aminco 2000C instrument in 10 mm optical pathway cells at 25°C. Oxidation of ferrocyanide *c* was measured in a dual-wavelength mode at 550 nm vs a reference wavelength at 535 or 540 nm. Turnover numbers (TN) for COX (e.g., 10 s<sup>-1</sup>) are expressed in electrons per second per cytochrome oxidase monomer, if not stated otherwise. The Ca<sup>2+</sup>-induced red shift of heme *a* absorption spectrum was measured in the SLM-Aminco 2000C spectrophotometer operated in a split beam mode. COX was pre-reduced by 5 mM ascorbate and 100 μM TMPD in the presence of 5 mM KCN that resulted in complete reduction of heme *a*. The difference spectra induced in the α-band of heme *a* by increasing concentrations of CaCl<sub>2</sub> in the presence of Ca<sup>2+</sup>-buffers were recorded. The amplitude of the derivative-shaped difference spectra at 613 nm minus 599–600 nm [16,19] was plotted vs the concentration of free Ca<sup>2+</sup>. The data were processed with OriginLab 7e software package (Microcal). The figures with the crystal structure of COX domains were prepared with the aid of PyMOL software.

## Results

Our conjecture was that the putative regulatory effect of Ca<sup>2+</sup> on COX activity, if in existence, would be more pronounced under the conditions of the enzyme turnover close to those in the respiring mitochondria. COX turnover in the respiring mitochondria (cf. [35,36]) differs from the standard cytochrome oxidase activity assays by at least two important parameters. First, in the

standard assays, turnover rate of cytochrome oxidase is close to V<sub>max</sub> (for bovine oxidase, ca. 200–600 s<sup>-1</sup> depending on pH), whereas in the mitochondria respiring on succinate or NADH-dependent substrates, COX turns over much slower, ca. 10 s<sup>-1</sup> or less, even in the fully uncoupled state. Second, in the standard assays, cytochrome *c* is kept almost fully reduced (e.g., by excess ascorbate and TMPD) and its redox potential, E<sub>h</sub>, is much lower than E<sub>m</sub>, whereas in mitochondria respiring with succinate or NADH-dependent substrates, cytochrome *c* is typically less than half-reduced in the steady-state [35,36]. Therefore, we have searched for effect of Ca<sup>2+</sup> on COX activity at slow turnover rates of the enzyme and at high redox potential of the electron donors.

## Inhibition of Purified COX by Ca<sup>2+</sup>

In the first series of experiments, slow aerobic turnover of purified bovine COX with ferrocyanide as the high-potential electron donor was studied in the presence of catalytic amount (40 nM) of cytochrome *c* [37]. The reaction decelerates with time mainly due to accumulation of ferricyanide raising further the redox potential, E<sub>h</sub>, of the donor. As shown in **Figure 2A**, the cytochrome *c*-catalyzed oxidation of ferrocyanide by COX is significantly inhibited by Ca<sup>2+</sup> (trace 2) but not by Mg<sup>2+</sup> (trace 3), and the inhibition is reversed by EGTA (**Figure 2B**). The same results were obtained in the control experiments in which 50 mM choline chloride in the reaction buffer was replaced by 50 mM KCl. No inhibition, but rather slight stimulation is observed with the wild type COX from *R. sphaeroides* (**Figure 2C**) containing tightly-bound Ca<sup>2+</sup> at the site. A small activating effect on ferrocyanide oxidation by the bacterial oxidase was also observed with Mg<sup>2+</sup> (not shown) and is most likely due to stimulation of direct interaction of ferrocyanide anion with the negatively charged electron entry site of the enzyme by divalent cations [38] (cf. the slight stimulation of the reaction by Mg<sup>2+</sup> in **Figure 2A**). The inhibition titrates with Ca<sup>2+</sup> according to a hyperbolic curve with K<sub>i</sub> of 0.9 μM and maximal inhibition of ~60% (**Figure 2D**).

The Ca<sup>2+</sup>-induced inhibition of COX is also observed with artificial electron donors, such as TMPD and ferrocyanide, in the absence of cytochrome *c* (**Figure 3AB**). The inhibition observed with TMPD (37±4%, 4 experiments) seems to be somewhat less than measured with the other electron donors tested (50–60%). However, it will increase to ~50% if corrected for ca. 25% of KCN-insensitive oxidation of TMPD in the presence of COX.

In the second set of experiments, effect of Ca<sup>2+</sup> on oxidation of excess ferrocyanide *c* by COX was studied in the absence of artificial redox compounds. A representative experiment is shown in **Figure 4**. Where indicated (“low turnover conditions”), the reaction rate was attenuated by increasing the ionic strength with high concentration of choline chloride and by including ferric cytochrome *c* in the medium. In a standard assay (“high turnover conditions”), no effect of Ca<sup>2+</sup> is observed (**Figure 4A**). However, if the conditions are set so as to decrease the rate of COX activity to ~5–10 s<sup>-1</sup> (**Figure 4B**), addition of Ca<sup>2+</sup> brings about ca. 2-fold inhibition of cytochrome *c* oxidation (**Figure 4B**, trace 3). The inhibitory effect of Ca<sup>2+</sup> at turnover rates below ~10 s<sup>-1</sup> has been documented for several large scale preparations of bovine CcO with but minor differences in the extent of inhibition among the preparations. In replicate experiments with the same sample of the enzyme at initial turnover rate of 6.2±0.05 s<sup>-1</sup>, the inhibition induced by 100 μM free calcium gives a value of 58±2% (15 experiments). No such effect is induced by Mg<sup>2+</sup> (**Figure 4B**, trace 2). Similarly to the results shown in **Figure 2**, the inhibitory effect of Ca<sup>2+</sup> on ferrocyanide *c* oxidation was reversed and prevented by excess EGTA and was not observed with COX

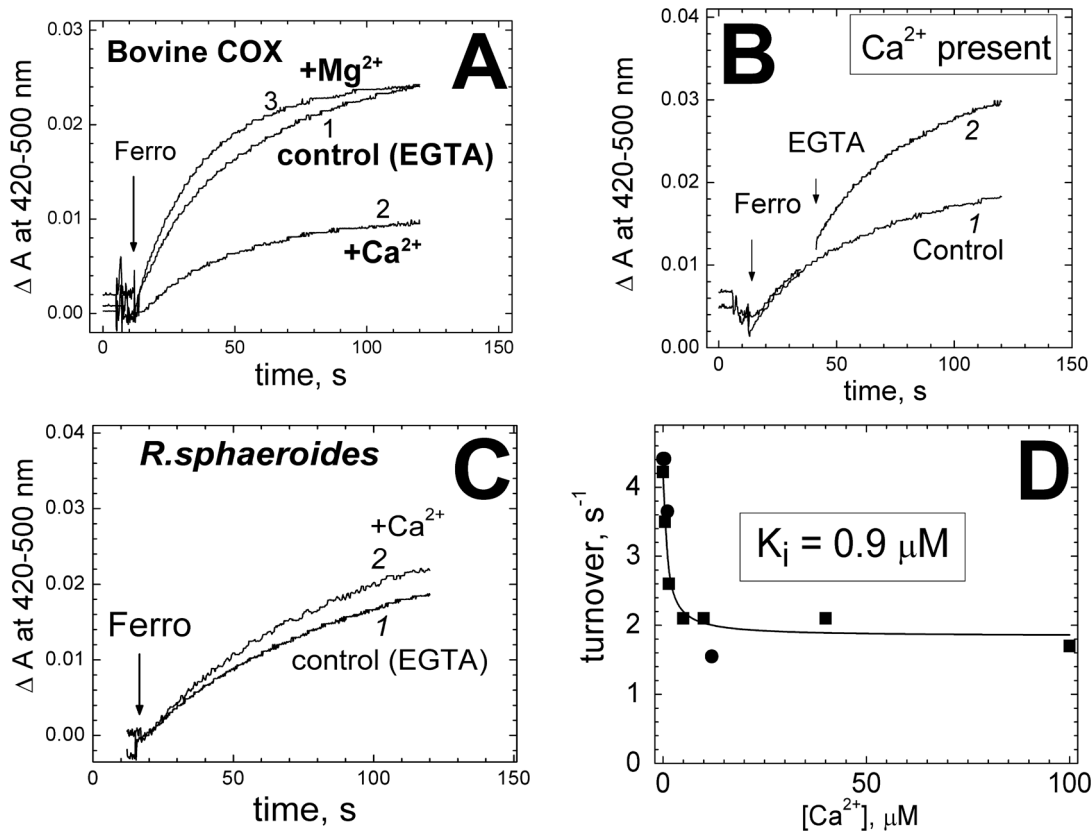


**Figure 2. Ca<sup>2+</sup> ions inhibit cytochrome *c*-catalyzed oxidation of ferrocyanide by cytochrome oxidase.** (A) 0.3 μM bovine COX in the basic medium (100 μM EGTA present) with 40 nM cytochrome *c*. Where indicated, 1 mM ferrocyanide (ferro) was added, and its oxidation to ferricyanide was followed spectrophotometrically at 420 nm vs the 500 nm reference. Trace 1, control recording; trace 2, +200 μM CaCl<sub>2</sub> (100 μM excess over EGTA); trace 3, +0.4 mM Mg<sup>2+</sup> (300 μM excess over EGTA). (B) Conditions, as in panel A, trace 2 (100 μM excess of CaCl<sub>2</sub> over EGTA). In trace 2, 300 μM EGTA has been added. (C) 0.2 μM wild-type COX from *R. sphaeroides*. Trace 1, control (100 μM EGTA). Trace 2, with 200 μM CaCl<sub>2</sub>. (D) Concentration dependence of the inhibition. Initial rate of ferrocyanide oxidation by COX (0.3 μM) is plotted vs concentration of free Ca<sup>2+</sup> buffered with 1 mM NTA (squares) or 1 mM BAPTA (circles). The curve corresponds to K<sub>i</sub> of 0.9 μM and maximal inhibition of 60%. doi:10.1371/journal.pone.0074436.g002

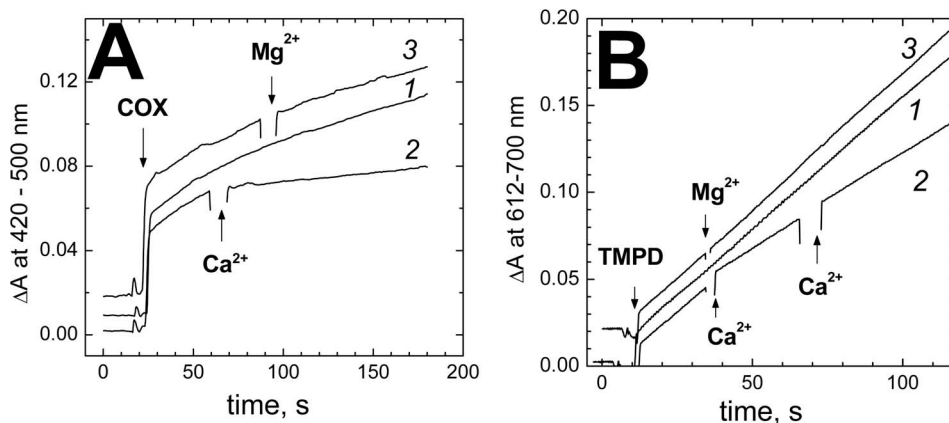


**Figure 3. Ca<sup>2+</sup> inhibits aerobic oxidation of artificial electron donors by COX.** (A) Oxidation of ferrocyanide. 0.2 mM ferrocyanide in the basic buffer pH 8.2, supplemented with 30 μg/ml of poly-L-lysine to stimulate reaction of COX with ferrocyanide anion [38]. Reaction is initiated by addition of 0.4 μM bovine COX and accumulation of ferricyanide is followed at 420 nm vs the 500 nm reference. Trace 1, control recording with no other additions; trace 2, 200 μM CaCl<sub>2</sub> added where indicated; trace 3, 400 μM MgSO<sub>4</sub> added instead of CaCl<sub>2</sub>. The initial upward jump of the traces is due to absorption of the added COX. (B) Oxidation of *N,N,N,N'*-tetramethyl-*p*-phenylenediamine. 0.15 μM bovine COX in the basic buffer. Where indicated, 0.1 mM reduced TMPD is added, and its oxidation to Wurster's Blue is followed spectrophotometrically at 612 nm vs the 700 nm reference. Trace 1, control recording with no additions; trace 2, 200 μM CaCl<sub>2</sub> added where indicated, note that the second addition does not induce any further inhibition; trace 3, 200 μM Mg<sup>2+</sup> added where indicated. The kinetics curves in the panels A and B are displaced arbitrarily on the ordinate axis for clarity. doi:10.1371/journal.pone.0074436.g003

from *R. sphaeroides* (data not included). The inhibitory effect of  $\text{Ca}^{2+}$  titrates according to a hyperbolic curve with the maximal inhibition of 50–60% and  $K_i$  of  $\sim 1.4 \mu\text{M}$  (Figure 4C, filled circles) in good agreement with the data on ferrocyanide oxidation (Figure 2D). The inhibition curve matches well induction of the red shift of heme *a* (Figure 4C, open circles).

$\text{Na}^+$  competes with  $\text{Ca}^{2+}$  for binding with COX [16,18,20], but does not affect significantly the activity of the enzyme (Figure 5A). For instance, under the experimental conditions at which 100  $\mu\text{M}$  free  $\text{Ca}^{2+}$  inhibits the reaction by  $58 \pm 2\%$ , addition of 50 mM  $\text{Na}^+$  (that is 12-fold the  $K_d$  value [16]), decreases the rate of ferrocyanide oxidation by  $9 \pm 5\%$  (5 experiments). At the same time, 50 mM  $\text{Na}^+$  largely prevents inhibition of the activity by  $\text{Ca}^{2+}$  (Figure 5A), and partial release of the inhibition imposed by  $\text{Ca}^{2+}$  could be observed (Figure 5B). These data are coherent with the observations that  $\text{Na}^+$  does not induce red shift of heme *a* [16,20] and does not affect  $E_m$  of heme *a* [39] but counteracts induction of these effects by  $\text{Ca}^{2+}$  ions.

Mutations in the conserved aspartate in the CBS of the bacterial oxidases from *P. denitrificans* or *R. sphaeroides* (D477A<sub>Pd</sub> or D485A<sub>Rs</sub>, homologous to D442 in bovine enzyme, cf. Figure 1B) release the tightly-bound bacterial  $\text{Ca}^{2+}$  from the CBS of the bacterial enzymes and allow to observe reversible binding of exogenous  $\text{Ca}^{2+}$  and  $\text{Na}^+$  with the site [14,15,17,18]. Interestingly, we found that  $\text{Ca}^{2+}$  does not affect ferrocyanide oxidation by either D485A mutant COX from *R. sphaeroides* (data not included) or D477A mutant COX from *P. denitrificans* (Figure 6). Thus, the inhibitory effect of calcium ions may be specific for the mammalian oxidase.

### Inhibition of the Cytochrome $c^{2+}$ Oxidase Activity in Mitochondria

The inhibitory effect of  $\text{Ca}^{2+}$  was further confirmed with COX in its native surroundings, i.e. in the mitochondrial membrane. To this end, we have measured spectrophotometrically ferrocyanide oxidation activity of mitochondria from several rat tissues. The outer membrane of the mitochondria was disrupted by Nagarse treatment [34] to make it permeable to cytochrome *c*. The Nagarse-treated mitochondria still showed respiratory control, therefore the experiments were carried out in the presence of CCCP, the uncoupler, and 1  $\mu\text{M}$  cyclosporin A to preclude  $\Delta\psi$ -driven  $\text{Ca}^{2+}$  accumulation in the mitochondrial matrix, swelling of the mitochondria and pore opening.

As shown in Figure 7A,  $\text{Ca}^{2+}$  inhibits oxidation of ferrocyanide by rat heart mitochondria about 2-fold. Similar results were obtained for mitochondria isolated from bovine heart (the Table). Stronger inhibition is observed with mitochondria from rat liver (Figure 7ABC, the Table). The inhibition is reversed by addition of excess EGTA (Figure 7B, trace 3). No inhibition was induced by  $\text{Mg}^{2+}$  (not shown). The inhibition of COX in liver mitochondria titrates with  $[I]_{50}$  of  $\sim 0.5 \mu\text{M}$  (Figure 3C, filled circles). The concentration dependence appears to be slightly sigmoidal, but it can be approximated reasonably well by a hyperbolic curve with  $K_i$  of  $0.75 \mu\text{M}$  and, within the experimental scatter, the data overlap with the titration of the  $\text{Ca}^{2+}$ -induced red shift of heme *a* (open circles,  $K_d \sim 0.5 \mu\text{M}$ ). Thus, like in the case of the purified bovine heart oxidase, the inhibition of COX activity in rat liver mitochondria correlates with calcium binding at the site responsible for the spectral shift of heme *a*. As with the soluble cytochrome oxidase, no significant effect of  $\text{Na}^+$  on the activity could be observed, but sodium ions prevented the  $\text{Ca}^{2+}$ -induced inhibition (data not shown).

The Table summarizes the inhibitory effects of  $\text{Ca}^{2+}$  on the COX activity of mitochondria from several rat tissues. The inhibition in mitochondria from the non-excitable tissues (liver and

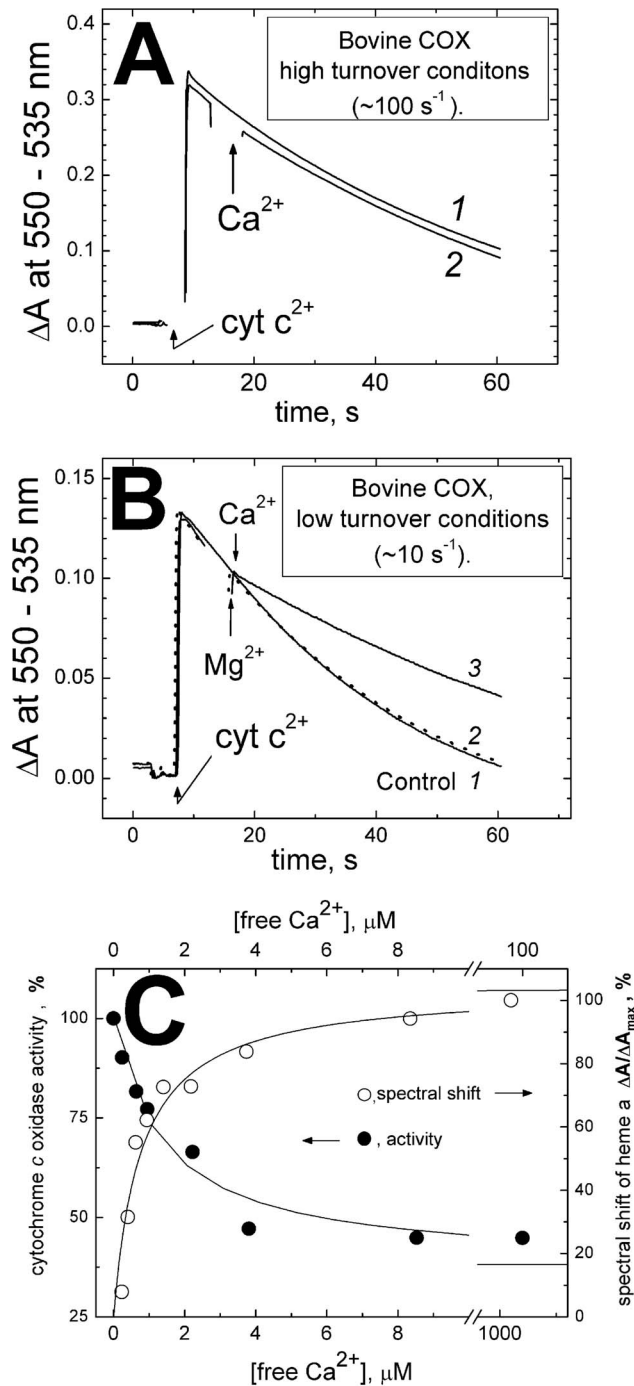


**Figure 4. Inhibition of the ferrocyanide *c* oxidase activity of bovine COX by  $\text{Ca}^{2+}$  ions.** (A) High-turnover conditions. 4 nM COX in the basic medium (with 50 mM choline chloride and 100  $\mu\text{M}$  EGTA). 18  $\mu\text{M}$  reduced cytochrome *c* is added and its subsequent oxidation is followed spectrophotometrically at 550 nm vs the 535 nm reference. Trace 1, control recording; trace 2, 200  $\mu\text{M}$   $\text{CaCl}_2$  added where indicated. (B) Low-turnover conditions. Conditions as in (A), but choline chloride concentration increased to 0.5 M and 18  $\mu\text{M}$  oxidized cytochrome *c* present in the buffer; COX concentration raised to 20 nM. Trace 1 (solid line), control recording; traces 2,3: where indicated, 0.4 mM  $\text{MgCl}_2$  (dashed line) or 200  $\mu\text{M}$   $\text{CaCl}_2$  (solid line) are added. (C) Titration of the  $\text{Ca}^{2+}$ -induced inhibition of COX activity and of the red shift of heme *a* spectrum. Cytochrome  $c^{2+}$  oxidation was measured as in Panel B, trace 1 at different concentrations of free calcium buffered with 5 mM HEDTA. The initial rates were used to build

the plot. Spectral shift measurements (see Materials and Methods) were made in the basic buffer with 2  $\mu\text{M}$  COX. Concentration of free  $\text{Ca}^{2+}$  was buffered with 5 mM HEDTA. The points are fitted by the curves: maximal inhibition,  $63 \pm 5\%$ ,  $K_i = 1.4 \pm 0.4 \mu\text{M}$ ; the spectral shift,  $\Delta A_{\text{max}} = 103\%$  of the highest experimentally observed  $\Delta A$  value taken as 100%;  $K_d = 0.77 \pm 0.19 \mu\text{M}$ .

doi:10.1371/journal.pone.0074436.g004

kidney) appears to be stronger than in the heart or skeletal muscle mitochondria. It is noted that the incomplete inhibition of COX by  $\text{Ca}^{2+}$  observed in the experiments may be explained, as usual, either by partial inhibition of the entire population of the enzyme or by complete inhibition of variable fraction of the enzyme (or both). More experiments are required to distinguish between these possibilities.

## Discussion

The principal finding of this work is that  $\text{Ca}^{2+}$  ions at concentrations of few  $\mu\text{M}$  inhibit mitochondrial cytochrome *c* oxidase, both in the soluble state and in the mitochondrial membrane. The inhibition is associated with  $\text{Ca}^{2+}$  binding at the special cation binding site of COX [10,11] located at the outer face of the mitochondrial membrane (cf. **Figure 1**) and, peculiarly, is observed only at low turnover rates of the enzyme.

### Why was the Inhibition not Observed Earlier?

There are several probable reasons. First, the COX activity assays are usually aimed to reveal the maximal turnover rate of the enzyme. As found in this work, at high concentrations of the fully reduced ferrocyanide *c* and turnover rate of  $\sim 10^2 \text{ s}^{-1}$  or higher at pH 8, no inhibitory effect of  $\text{Ca}^{2+}$  is observed (e.g., **Figure 4A**). Second, the effect of  $\text{Ca}^{2+}$  is characterized by rather high affinity of the enzyme for the cation ( $K_i \sim K_d \sim 10^{-6} \text{ M}$ ). The reaction media used in experiments may easily contain some 5–10  $\mu\text{M}$  of adventitious  $\text{Ca}^{2+}$  unless special precautions are taken. Therefore, the CBS of COX may be saturated with  $\text{Ca}^{2+}$

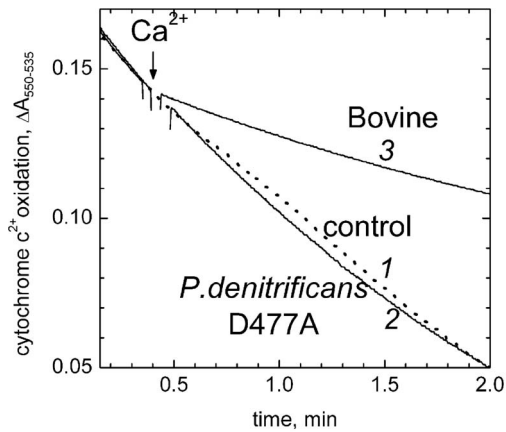


**Figure 6.  $\text{Ca}^{2+}$  does not inhibit cytochrome  $c^{2+}$  oxidase activity of D477A mutant COX from *P.denitrificans*.** D477A mutant COX (1.5 nM) in the basic medium with 0.4 M choline chloride. Oxidation of 10  $\mu\text{M}$  reduced cytochrome *c* is followed spectrophotometrically in a dual-wavelength mode at 550 nm vs the 535 nm reference. Trace 1 (dotted line), control recording with no calcium added; trace 2, 200  $\mu\text{M}$   $\text{CaCl}_2$  added where indicated. Trace 3, the same conditions as in trace 2 but with 2.5 nM bovine heart COX.

doi:10.1371/journal.pone.0074436.g006

already before addition of exogenous calcium. In order to control free  $\text{Ca}^{2+}$  concentration in the  $\mu\text{M}$  range,  $\text{Ca}^{2+}$  buffers have to be used which was not often the case in the past works on  $\text{Ca}^{2+}$  interaction with COX (e.g. [12,19,40]). Third,  $\text{Ca}^{2+}$  binding with COX is antagonized by  $\text{Na}^+$ , concentration of which in the buffers was rarely specifically controlled. Combination of these factors can readily explain why the inhibitory effect of  $\text{Ca}^{2+}$  on the cytochrome *c* oxidase activity was not noticed earlier.

As a matter of fact, scattered evidence for inhibition of the mitochondrial respiration by micromolar  $\text{Ca}^{2+}$  can be found in the literature (e.g., cf. Fig. 4 of ref. [27], Table 1 in ref. [41], ref. [42]),

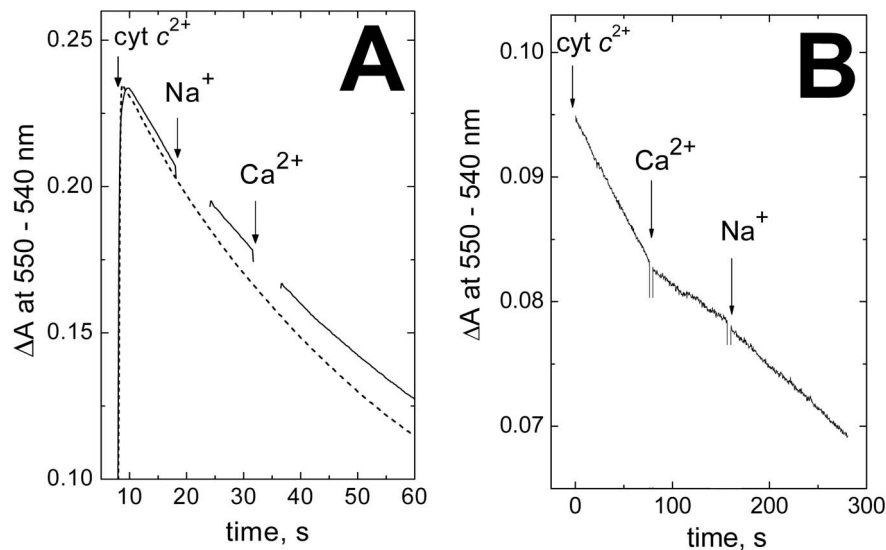


**Figure 5.  $\text{Na}^+$  ions counteract the  $\text{Ca}^{2+}$ -induced inhibition of cytochrome *c* oxidase activity of bovine COX.** (A) Bovine COX (30 nM) in the basic medium with 0.4 M choline chloride and 15  $\mu\text{M}$  oxidized cytochrome *c*. The reaction is initiated by addition of 15  $\mu\text{M}$  ferrocyanide *c* and oxidation of  $c^{2+}$  is followed in a dual-wavelength mode at 550 nm vs the 540 nm reference wavelength. Dashed line, control recording (no additions). Solid line, 50 mM NaCl and 200  $\mu\text{M}$   $\text{CaCl}_2$  (100  $\mu\text{M}$  excess over EGTA) are added where indicated. (B) Bovine COX (1.3 nM) in the basic medium with 0.4 M choline chloride and with no oxidized cytochrome *c*. Reaction is initiated by addition of 6  $\mu\text{M}$  ferrocyanide *c*. Other additions, as in (A).

doi:10.1371/journal.pone.0074436.g005

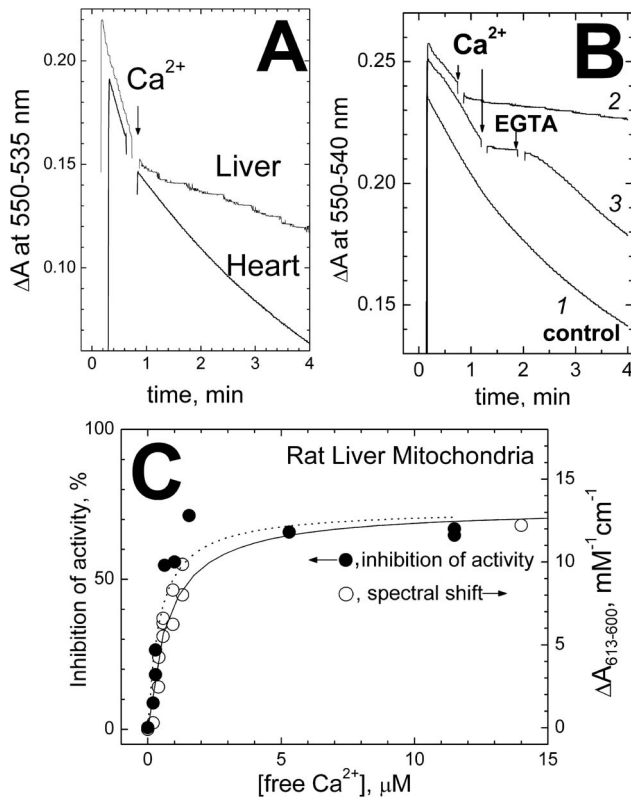


**Figure 7.  $\text{Ca}^{2+}$ -induced inhibition of ferrocyanide *c* oxidase activity in mitochondria.** (A) Rat liver (1.3 mg protein/ml) or rat heart mitochondria (0.6 mg protein/ml) in the medium containing 0.25 M sucrose, 50 mM HEPES/tris pH 8.0, 0.4 M choline chloride, 100  $\mu\text{M}$  EGTA, and also 1  $\mu\text{M}$  cyclosporine A and 1  $\mu\text{M}$  the uncoupler, CCCP. 15  $\mu\text{M}$  of the reduced cytochrome *c* is added and its oxidation is followed at 550 nm vs the 535 nm reference.  $\text{Ca}^{2+}$  addition, 200  $\mu\text{M}$ . (B) Rat liver mitochondria. Conditions, as in trace 1 of panel A. Additions:  $\text{CaCl}_2$ , 200  $\mu\text{M}$ ; EGTA, 300  $\mu\text{M}$ . The traces in the Panels A,B have been displaced arbitrarily on the ordinate scale for clarity. (C) Concentration dependences of the  $\text{Ca}^{2+}$ -induced inhibition of COX and spectral shift of heme *a* in rat liver mitochondria. Cytochrome  $\text{c}^{2+}$  oxidation was measured as in Figure 7B, trace 1 at different concentrations of free calcium buffered with 5 mM HEDTA or 5 mM NTA. The initial slopes of the kinetic curves were used to build the plot. The data have been approximated by a hyperbolic curve (solid line) with the maximal inhibition of 74% and  $K_i = 0.76 \mu\text{M}$ . The  $\text{Ca}^{2+}$ -induced spectral shift of the reduced heme *a* was measured in an SLM-Aminco-2000C spectrophotometer (see Materials and methods). To decrease light scattering, the mitochondria (10–15 mg protein/ml) were treated with 1% dodecyl maltoside. The data are approximated by a curve (dashed line) with  $\Delta A_{613-600}(\text{max}) = 13 \text{ mM}^{-1} \text{ cm}^{-1}$ , and  $K_d = 0.56 \mu\text{M}$ . doi:10.1371/journal.pone.0074436.g007

and the inhibition may be attributed, at least partly, to the inhibitory effect of the cation on the mitochondrial COX. (Take notice that the specific activity of the mitochondrial COX was determined in ref. [42] under high turnover conditions at which the inhibition of COX itself by  $\text{Ca}^{2+}$  would not be observed).

### The Mechanism of the $\text{Ca}^{2+}$ -induced Inhibition of COX

Several possible explanations may be considered.

(i) **Effect of  $\text{Ca}^{2+}$  on cytochrome *c* binding with COX.** Binding of cytochrome *c* with COX is essentially electrostatic, so one could propose that  $\text{Ca}^{2+}$  competes with cytochrome *c* for the anionic binding site at  $\text{Cu}_A$ . However, the observed inhibitory effect of  $\text{Ca}^{2+}$  requires the cation binding at

**Table 1. Inhibition of the mitochondrial cytochrome *c* oxidase activity by  $\text{Ca}^{2+}$ .**

	Inhibition, %			
	Heart	Skeletal muscle	Liver	Kidney
Rat mitochondria	50 $\pm$ 5	60 $\pm$ 5	80 $\pm$ 2	76 $\pm$ 4
Bovine mitochondria	57 $\pm$ 4	–	–	–

Oxidation of 15  $\mu\text{M}$  ferrocyanide *c* by mitochondria from different tissues (0.5–1.5 mg protein/ml) was followed spectrophotometrically under low-turnover conditions as described in “Materials and Methods” and legend to Figure 7. The data correspond to inhibition induced by addition of excess  $\text{Ca}^{2+}$  (200  $\mu\text{M}$  on the background of 100  $\mu\text{M}$  EGTA). The data are average  $\pm$  SE for 3–5 measurements.

doi:10.1371/journal.pone.0074436.t001

the specific Cation Binding Site separate from the cytochrome *c* docking site; the effect is not mimicked by  $\text{Mg}^{2+}$  and is not observed with the bacterial oxidases. Furthermore, the inhibition of bovine oxidase by  $\text{Ca}^{2+}$  can be observed with the artificial electron donors - anionic ferrocyanide (Figure 3A) and uncharged TMPD (Figure 3B). Therefore, the explanation (i) is not likely.

(ii) **Modulation of intraprotein electron transfer due to a shift of heme *a* midpoint redox potential.** According to our initial hypothesis [43], the inhibition of COX by  $\text{Ca}^{2+}$  could be related to a positive shift of  $E_m$  of heme *a* induced by the cation [18,29,39]. However, we found that  $\text{Ca}^{2+}$  does not inhibit activity of mutant COX from *R. sphaeroides* (D485A) or *P. denitrificans* (D477A) (cf. Figure 6). These mutant oxidases are fully active and bind  $\text{Ca}^{2+}$  at the CBS reversibly in much the same way as bovine oxidase [14,17,18]. Moreover, a  $\text{Ca}^{2+}$ -induced positive shift of  $E_m$  of heme *a* by 40–50 mV is observed with D477A oxidase from *P. denitrificans* that is stronger than the 15–20 mV shift found with the bovine COX ([39], paper in preparation). Nevertheless, there is no inhibition of the mutant D477A oxidase by calcium ions (Figure 6). Thus, the inhibitory effect of  $\text{Ca}^{2+}$  is not likely to be a simple consequence of  $\Delta E_m$  of heme *a* and the inhibition may be specific for the mammalian COX.

(iii) **Inhibition of  $\text{H}^+$  transfer through the proton conducting pathway H.** As discussed in [15,16,18,21,44] the cation binding site in COX is adjacent to the exit part of the so-called “proton-conducting pathway H” or, simply, the “H-channel” described by Yoshikawa, Tsukihara and collaborators [11,45] (Figure 1A, Figure 8). The H-channel has been proposed to be involved in translocation of the pumped protons by bovine heart COX and the proposal has received some experimental support [11,45–50]. Alternative functions of the H-channel were considered in [15,18,51]. It was proposed that the channel may carry out controlled dissipation of proton gradient [15,18] being involved in the so-called “mild uncoupling” of mitochondria [52], or function as a “dielectric channel” [51] facilitating electron transfer through heme *a*.

Crystal structure of the  $\text{Ca}^{2+}$ -bound CBS in bovine COX has not been published yet, but it was modeled [17,18] assuming similarity between coordination of  $\text{Ca}^{2+}$  and  $\text{Na}^+$  in bovine COX and taking into account the resolved structure of the  $\text{Ca}^{2+}$ -loaded site in the bacterial oxidases (refs. [14,15], PDB entry 1M56). Among the other groups, the cation is coordinated by the backbone carbonyl function of S441 [11,44] (cf. Figure 1B, Figure 8). This serine located in a cytoplasmic loop connecting transmembrane helices XI and XII of subunit I is conserved in the oxidases from higher animals (annelid worms and higher) but is

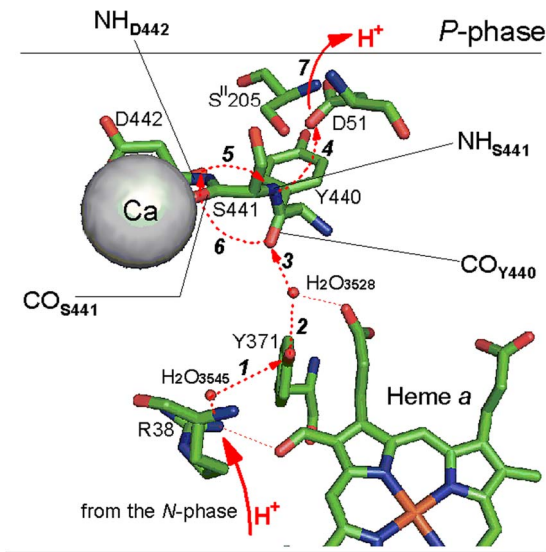


**Figure 8. Interaction of  $\text{Ca}^{2+}$  with the exit of proton channel H in bovine heart oxidase.** Structure of the exit part of the H-channel is shown based on the oxidized COX crystal structure, PDB entry 1V54. All the groups shown belong to subunit I (polypeptide A) except for S<sup>II</sup>205 from subunit II (polypeptide B). The scheme gives a scenario of proton transfer combined from refs. [44,45,49]. Proton trajectory is depicted by red arrows and sequence of the proton transfer steps is indicated by numbers. Oxidation of heme *a* by the binuclear site brings about a conformational change that unlocks the H-channel below the heme [46] (cf. [50] for an alternative proposal) and pumped proton arrives to the guanidine group of R38 from the *N*-aqueous phase (step 1) via the input part of the H-channel (cf. **Figure 1A**); it travels further via the R38-bound H<sub>2</sub>O<sub>3545</sub> (that has then to shift closer to Y371), OH group of Y371 and H<sub>2</sub>O<sub>3528</sub> to finally protonate the backbone carbonyl group of Y440 (steps 2–4). The carbonyl function C=O<sub>Y440</sub> protonated, makes the -NH<sub>S441</sub> acidic (imidic acid) and allows for its facile spontaneous deprotonation by carboxylate of D51 (step 5), converting the S441-Y440 peptide bond to the enol form. The protonated state of D51 is then stabilized by multiple hydrogen bonding to S<sup>II</sup>205 and S441. As proposed in [44], the enol form of the S441-Y440 peptide bond returns to the initial keto form (the notorious proton transfer via the peptide bond S441-Y440 [44,45,49]) actually in two steps. First, the deprotonated enolic=N<sub>S441</sub> receives proton from the backbone -NH of D442 (step 6, the rate limiting stage of the entire process), which is followed by facile reprotonation of -N<sub>D442</sub> by the protonated backbone C-OH<sub>Y440</sub> (step 7) returning the latter to the initial carbonyl state. Upon subsequent reduction of heme *a*, D51 undergoes reorientation associated with loss of the stabilizing hydrogen bonding to S<sup>II</sup>205 and, hence, decreased proton affinity, so that its carboxylic group releases the proton to the *P*-phase (step 8).  $\text{Ca}^{2+}$  coordinates to the backbone carbonyl oxygen of S441, and also makes a bond with the carboxylate of D442 via intercalated fixed water molecule (hidden behind the Ca ion in this projection of the structure, cf. H<sub>2</sub>O<sub>3544</sub> in **Figure 1B** and see ref. [14]). As discussed in the text,  $\text{Ca}^{2+}$  is expected to inhibit proton transfer through the exit part of the H-channel and, accordingly, to impede the proton transfer-coupled electron transfer by COX.

doi:10.1371/journal.pone.0074436.g008

absent from COX of bacteria, yeast, fungi or higher plants (refs. [16,53], bioinformatics search made in our group by N.Tretyakova). According to the proton pumping mechanism considered by Yoshikawa and collaborates [47,54], S441 plays a key role in proton conduction through the exit part of the H-channel (**Figure 8**). First, its backbone amide group is proposed to be involved in delivery of the pumped proton to D51 via the peptide bond Y440-S441 [47,48]. Second, the side chain of S441 makes a hydrogen bond to D51, a residue that gates release of the pumped

$\text{H}^+$  to cytoplasm changing its conformation upon reduction of heme *a* [11,49]. Besides the interaction with S441,  $\text{Ca}^{2+}$  is likely to strongly interact with the carboxylate of D442 via intercalated fixed water [14,18], whereas the amide function of D442 is proposed to participate in the two-step  $\text{H}^+$ -transfer across the Y440-S441 peptide bond (**Figure 8**, ref. [44]).

Binding of  $\text{Ca}^{2+}$  at the CBS may be envisaged to inhibit proton transfer through the exit part of the H-channel. First, there are positively charged intermediates, such as hydronium cation H<sub>3</sub>O<sup>+</sup><sub>3528</sub> or the imidic acid state HOC=NH<sup>+</sup> of the Y440-S441 peptide bond, that are postulated to be formed along the  $\text{H}^+$ -transfer pathway through the exit part of the H-channel [44,45,49,55]. The extra positive charge introduced by  $\text{Ca}^{2+}$  should hamper generation of such intermediates in vicinity of the cation. Second, and perhaps more important, the geometry of the bonds and distribution of the electronic clouds in the Y440-S441-D442 backbone segment are finely tuned in order to allow for the two-step mechanism of  $\text{H}^+$  transfer “through the Y440-S441 peptide bond” involving the Y440-S441 and S441-D442 peptide groups [44,55]. Strong interactions of  $\text{Ca}^{2+}$  with the backbone carbonyl of S441 and with the side-chain of D442 are envisaged to distort the optimized structure and to make the site more rigid, thus raising the activation energy of the D442 backbone amide-assisted  $\text{H}^+$ -transfer through the Y440-S441 peptide bond. Therefore,  $\text{Ca}^{2+}$  binding at the CBS is expected to inhibit intramolecular transfer of the protons through the exit of the H-channel and, accordingly, to hinder the redox activity of the enzyme coupled to the proton transfer.

It is tempting to speculate that in the bacterial A-class oxidases [13] in which the H-channel is partly conserved [47] but is not involved in proton pumping [56,57], the tightly-bound calcium at the homologous CBS [10,14,15] may serve as a plug preventing backward proton leak through the idle H-pathway. The same role of locking securely the non-operative proton pathway can be proposed for the tightly-bound  $\text{Ca}^{2+}$  in the *ccb*<sub>3</sub> oxidases, where the cation binds with the critical residues gating connection to the exit of the D-channel-associated proton pumping pathway that works in the A-type oxidases but is non-operative in the C-type *ccb*<sub>3</sub> oxidases [58,59].

### Why is the $\text{Ca}^{2+}$ -induced Inhibition Observed Only at Low Turnover Rates?

As the molecular mechanism of the calcium-induced inhibition of COX is not yet clear, there is no obvious answer to the question. In particular, it is difficult to discriminate between two interrelated factors: slow turnover per se and low steady-state reduction level of the redox centers in the enzyme. Preliminary experiments in which the rate of COX turnover was varied at a constant redox potential of cytochrome *c* (a 1:1 mixture of the ferrous and ferric forms) indicate that the turnover rate may be itself important (**Figure S1**), but it does not exclude the role of redox potential of cytochrome *c*. Much more experiments are required to clarify the quantitative aspects of the  $\text{Ca}^{2+}$ -induced inhibition. In any case, it is worth noting that, firstly, the low turnover rates at which the inhibition is observed most clearly ( $\sim 10 \text{ s}^{-1}$  or less) are close to typical turnover rates of COX in the respiratory chain of mitochondria (ca.  $100 \text{ ng-at O}_2 \cdot \text{min}^{-1} \cdot (\text{mg protein})^{-1}$ , i.e.  $\sim 10 \text{ s}^{-1}$ , assuming 0.3 nmol of *aa*<sub>3</sub> per mg of protein of heart mitochondria [35]). Secondly, at oxygen concentrations above 1  $\mu\text{M}$ , cytochrome *c* is only partly reduced in the actively respiring mitochondria (typically, 25–50% [35,36]) as in our experiments, while it is almost fully reduced under the conditions of the standard COX assays. Therefore, the parameters of COX turnover under which the calcium inhibitory effect is observed



are more relevant to physiological mode of the enzyme operation than those during the conventional conditions of COX activity assays. Different modes of COX operation at high- and low-turnover conditions in the cell have been discussed in the literature (reviewed, [60–63]) and the oxidase that turns over slowly is more susceptible to regulation by nucleotides similarly to modulation of the activity by calcium ions in this work. Higher susceptibility of COX to inhibition under low-turnover conditions has been described also for the inhibitory effect of Zn<sup>2+</sup> ions [40,64,65]. Interestingly, S441 is located in a sequence RRYS that is a canonical target for protein kinase A, which may be a one more interesting aspect of the regulatory function of the CBS [15,53,60].

### Physiological Significance of the Ca<sup>2+</sup>-induced Inhibition of COX

It remains an open question, to which extent the Ca<sup>2+</sup>-induced inhibition of COX described in this work may be involved in regulation of oxidative phosphorylation by the cation under physiological conditions. Typical cytoplasmic concentration of free Ca<sup>2+</sup> under resting conditions is 0.1–0.2 μM [23], i.e. below K<sub>d</sub> ~1 μM of Ca<sup>2+</sup> binding with COX. Moreover, if competition of Ca<sup>2+</sup> with Na<sup>+</sup> is taken into account [16,20], then at 5–10 mM of cytoplasmic Na<sup>+</sup> [66] the effective K<sub>d</sub> for Ca<sup>2+</sup> binding with COX should rise to ~10<sup>-5</sup> M [16,18]. Therefore under the resting conditions, the cation binding site of COX is expected to be occupied by Na<sup>+</sup> (K<sub>d</sub> ~ 10<sup>-3</sup> M [16]) that does not inhibit the enzyme. However, during release of Ca<sup>2+</sup> from endoplasmic reticulum or upon its entry from the extracellular stores in response to various stimuli, local concentrations of Ca<sup>2+</sup> in microdomains near mitochondria “can readily reach many tens of micromolar” [67,68] or even 100 μM [69], so that transient displacement of Na<sup>+</sup> and binding of Ca<sup>2+</sup> to COX during the spikes may well take place. The major potential consequences of such transient binding could be as follows.

#### (i) Inhibition of the Mitochondrial Respiration

Ca<sup>2+</sup> enhances oxidative phosphorylation as it is taken up inside mitochondria and activates there several Krebs cycle dehydrogenases (reviewed, [24,25,70]) and perhaps some respiratory chain cytochrome complexes [71]. Ca<sup>2+</sup> also acts from the outside of mitochondria by activating the *aralar*- and *citrim*-type substrate transporters in mitochondria from some tissues [26,27,70]. Our data indicate that in addition, the cytoplasmic (extramitochondrial) Ca<sup>2+</sup> ions may slow down mitochondrial respiration by direct inhibition of cytochrome *c* oxidase (cf. [27,41,42]).

(ii) *Stimulation of Reactive Oxygen Species (ROS) production.* Activation of the dehydrogenases and concomitant inhibition of COX should act synergistically in increasing the reduction of the respiratory chain carriers at given NAD(P)H/NAD(P)<sup>+</sup> and GSH/GSSG ratios in the mitochondrial matrix. In this way Ca<sup>2+</sup> is expected to stimulate ROS production by the respiratory chain (cf. [72] and refs. therein). Transient increase in ROS production may be in its turn part of intracellular signal transmission cascade in response to various stimuli.

(iii) *Modulation of calcium uptake by mitochondria.* Ca<sup>2+</sup> is taken up actively by respiring mitochondria via the so-called calcium uniporter, a highly specific Ca<sup>2+</sup> channel, down the Δψ formed by the respiratory chain ([66,73,74] and refs. therein). Inhibition of COX and hence of the entire respiratory chain by Ca<sup>2+</sup> is expected to slow down the respiration-driven Ca<sup>2+</sup> uptake and to attenuate accumulation of Ca<sup>2+</sup> in the mitochondrial matrix. It is noted that at cytoplasmic concentrations of Na<sup>+</sup>, affinity of COX for Ca<sup>2+</sup> virtually coincide with the effective “K<sub>m</sub>” of the mitochondrial calcium uniporter (ca. 10 μM [74]). Therefore,

cytochrome oxidase and the calcium uniporter are expected to respond to changes in cytoplasmic [Ca<sup>2+</sup>] within the same concentration range, but perhaps with different time constants, as there is a significant lag in activation of the calcium uniporter. This may be an interesting object for modeling.

In the excitable tissues like heart or skeletal muscle, the Ca<sup>2+</sup>-induced inhibition of COX is moderate (~2-fold). A likely role of the inhibition might consist in damping the effects of the periodical [Ca<sup>2+</sup><sub>free</sub>] spikes in the cytoplasm [68,70]; such damping would protect mitochondria from overloading with Ca<sup>2+</sup> during the spikes. In the non-excitabile tissues, mitochondria that are able to suck in rapidly calcium released to the cytoplasm from the endoplasmic reticulum cisterns or delivered from the extracellular stores, are active players in the Ca<sup>2+</sup>-mediated signal transmission and participate in “shaping in time and space” the cytoplasmic Ca<sup>2+</sup> signals [23,75,76]. Significant inhibition of COX in liver or kidney mitochondria by Ca<sup>2+</sup> could then be involved in modulation of the multiple regulatory pathways in which mitochondria interfere with the cellular response to Ca<sup>2+</sup>.

### Conclusions

1. The direct inhibitory effect of Ca<sup>2+</sup> on mammalian cytochrome oxidase is an important novel factor potentially involved in regulation of oxidative phosphorylation, mitochondrial ROS production and intracellular transmission of the calcium signals.

2. Location of the calcium binding site near the exit of the so-called proton conducting pathway H along with the specific inhibitory effect of Ca<sup>2+</sup> on the mammalian, but not on the bacterial, cytochrome oxidases, favour functional significance of the “H-channel” in cytochrome oxidase from mammalian mitochondria. Ca<sup>2+</sup> may be proposed to be a physiological specific inhibitor of the H-channel, whatever the function of the channel is.

### Supporting Information

**Figure S1** The calcium-induced inhibition of cytochrome *c* oxidase at different concentrations but constant redox potential of cytochrome *c*. The reaction mixture contained 50 mM tris-MES buffer, pH 8, with 0.4 M choline chloride, 0.05% DM, 100 μM EGTA and 1:1 mixture of the oxidized and reduced forms of cytochrome *c* at concentrations indicated (1–55 μM of each). The cytochrome oxidase reaction was initiated by addition of 6 nM purified bovine COX, and oxidation of cytochrome *c*<sup>2+</sup> was followed spectrophotometrically in a dual-wavelength mode at 550 nm vs the 535 nm reference. Where indicated, 200 μM Ca<sup>2+</sup> (100 μM excess over EGTA) was also present. The curves are drawn through the points to guide the eye. *Is turnover rate an essential factor that determines cytochrome *c* oxidase sensitivity to inhibition by Ca<sup>2+</sup>?* In a pilot experiment shown in **Figure S1**, concentration of cytochrome *c* was varied to change the cytochrome *c* oxidase reaction rate, while the redox potential was kept constant by using equimolar mixture of the reduced and oxidized cytochrome *c* for each point. It can be seen that the curves in the absence and in the presence of calcium tend to converge as the reaction rate increases. For instance, the inhibition induced by Ca<sup>2+</sup> is 57% at the lowest rate of electron transfer (1.2 s<sup>-1</sup>), 44% at 6.1 s<sup>-1</sup> and 21% at 12 s<sup>-1</sup>. In agreement with the data in **Figure 4A**, no inhibition at all was observed at turnover rate of 105 s<sup>-1</sup>; the latter point (not included in **Figure S1**) was measured with this sample of COX in a separate experiment with 15 μM ferrocytochrome as the electron donor but without ferric cytochrome *c* and at choline concentration of 50 mM. Results of the experiment confirm that the turnover rate is indeed an essential factor affecting the

sensitivity of COX to inhibition by calcium. Conceivably, the data do not exclude contribution of other factors, such as redox potential. It is noted that the dependencies in are to be considered as preliminary data and apply just to one of the several COX samples studied in this work. The exact profile for the  $\text{Ca}^{2+}$ -induced inhibition as a function of turnover rate may vary for different preparations. (E.g., in the preparation for which most of the data presented in the paper have been obtained, inhibition of  $58 \pm 2\%$  was observed at turnover rate of  $6 \text{ s}^{-1}$ , rather than  $44\%$  as in **Figure S1**). As we do not know yet all the parameters affecting the  $\text{Ca}^{2+}$ -sensitivity of COX, much more experiments are required for quantitative description of the phenomenon. (TIF)

## References

- Ferguson-Miller S, Babcock GT (1996) Heme/Copper Terminal Oxidases. *Chem Rev* 7: 2889–2907.
- Brzezinski P, Gennis RB (2008) Cytochrome c oxidase: exciting progress and remaining mysteries. *J Bioenerg Biomembr* 40: 521–531.
- Belevich I, Verkhovsky MI (2008) Molecular Mechanism of Proton Translocation by Cytochrome c Oxidase. *Antioxidants and Redox Signaling* 10: 1–29.
- Einarsdottir O, Caughey W (1985) Bovine heart cytochrome c oxidase preparations contain high affinity binding sites for magnesium as well as for zinc, copper, and heme iron. *Biochem Biophys Res Commun* 129: 840–847.
- Iwata S, Ostermeier C, Ludwig B, Michel H (1995) Structure at 2.8 Å Resolution of Cytochrome c Oxidase from *Paracoccus denitrificans*. *Nature* 376: 660–669.
- Tsukahara T, Aoyama H, Yamashita E, Tomizaki T, Yamaguchi H, et al. (1995) Structures of Metal Sites of Oxidized Bovine Heart Cytochrome c Oxidase at 2.8 Å. *Science* 269: 1069–1074.
- Sharpe MA, Qin L, Ferguson-Miller S (2005) Proton entry, exit and pathways in cytochrome oxidase: insight from conserved water. In: Wikstrom M, editor. *Biophysical and structural aspects of bioenergetics*. Norfolk: RSC Publishing. 26–52.
- Sharpe MA, Krzyaniak MD, Xu S, McCracken J, Ferguson-Miller S (2009) EPR Evidence of Cyanide Binding to the Mn(Mg) Center of Cytochrome c Oxidase: Support for  $\text{Cu}_A$ -Mg Involvement in Proton Pumping. *Biochemistry* 48: 328–335.
- Sugitani R, Stuchebrukhov AA (2009) Molecular dynamics simulation of water in cytochrome c oxidase reveals two water exit pathways and the mechanism of transport. *Biochim Biophys Acta* 1787: 1140–1150.
- Ostermeier C, Harrenga A, Ermler U, Michel H (1997) Structure at 2.7 Å resolution of the *Paracoccus denitrificans* two-subunit cytochrome c oxidase complexed with an antibody Fv fragment. *Proc Natl Acad Sci USA* 94: 10547–10553.
- Yoshikawa S, Shinzawa-Itoh K, Nakashima R, Yaono R, Inoue N, et al. (1998) Redox-Coupled Crystal Structural Changes in Bovine Heart Cytochrome c Oxidase. *Science* 280: 1723–1729.
- Wikstrom M, Saari H (1975) A spectral shift of heme a induced by calcium ions. *Biochim Biophys Acta* 408: 170–179.
- Pereira MM, Santana M, Teixeira M (2001) A novel scenario for the evolution of haem-copper oxygen reductases. *Biochim Biophys Acta* 1505: 185–208.
- Pfützner U, Kirichenko A, Konstantinov AA, Mertens M, Wittershagen A, et al. (1999) Mutations in the  $\text{Ca}^{2+}$ -binding site of the *Paracoccus denitrificans* cytochrome c oxidase. *FEBS Lett* 456: 365–369.
- Lee A, Kirichenko A, Vygodina T, Siletsky SA, Das TK, et al. (2002)  $\text{Ca}^{2+}$ -binding site in *Rhodobacter sphaeroides* cytochrome c oxidase. *Biochemistry* 41: 8896–8898.
- Kirichenko A, Vygodina TV, Mkrtychyan HM, Konstantinov AA (1998) Specific cation-binding site in mammalian cytochrome c oxidase. *FEBS Lett* 423: 329–333.
- Riistama S, Laakkonen L, Wikstrom M, Verkhovsky MI, Puustinen A (1999) The Calcium Binding Site in Cytochrome  $a_3$  from *Paracoccus denitrificans*. *Biochemistry* 38: 10670–10677.
- Kirichenko AV, Pfützner U, Ludwig B, Soares CM, Vygodina TV, et al. (2005) Cytochrome c oxidase as a calcium binding protein. Studies on the role of a conserved aspartate in helices XI–XII cytoplasmic loop in cation binding. *Biochemistry* 44: 12391–12401.
- Saari H, Pentilla T, Wikstrom M (1980) Interaction of  $\text{Ca}^{2+}$  and  $\text{H}^+$  with heme A in cytochrome oxidase. *J Bioenerg Biomembr* 12: 325–338.
- Mkrtychyan H, Vygodina T, Konstantinov AA (1990)  $\text{Na}^+$ -induced Reversal of the  $\text{Ca}^{2+}$ -dependent Red Shift of Cytochrome a. Is there a Hydronium Output Well in Cytochrome c Oxidase? *Biochem Internat* 20: 183–190.
- Marechal A, Iwaki M, Rich PR (2013) Structural Changes in Cytochrome c Oxidase Induced by Binding of Sodium and Calcium Ions: An ATR-FTIR Study. *J Am Chem Soc* 135: 5802–5807.
- Evenas J, Malmendal A, Forsen S (1998) Calcium. *Curr Opin Chem Biol* 2: 293–302.
- Clapham DE (2007) Calcium Signalling. *Cell* 131: 1047–1058.
- Denton RM (2009) Regulation of mitochondrial dehydrogenases by calcium ions. *Biochim Biophys Acta* 1787: 1309–1316.
- Tarasov AI, Griffiths EJ, Rutter GA (2012) Regulation of ATP production by mitochondrial  $\text{Ca}^{2+}$ . *Cell Calcium* 52: 28–35.
- Satrústegui J, Pardo B, Del Arco A (2007) Mitochondrial transporters as novel targets for intracellular calcium signaling. *Physiol Rev* 87: 29–67.
- Gellerich FN, Gizatullina Z, Trumbeckaite S, Nguyen NP, Pallas T, et al. (2010) The regulation of OXPHOS by extramitochondrial calcium. *Biochim Biophys Acta* 1797: 1018–1027.
- Vygodina TV, Konstantinov AA (2010)  $\text{Ca}^{2+}$ -induced inhibition of the mammalian cytochrome c oxidase. *Biochim Biophys Acta* 1797: 102.
- Konstantinov AA (2010) Cytochrome c oxidase: Electrogenic mechanism and regulation by calcium ions. *Biochim Biophys Acta* 1797 Suppl: 92.
- Fowler LR, Richardson SH, Hatefi Y (1962) A rapid method for the preparation of highly purified cytochrome oxidase. *Biochim Biophys Acta* 64: 170–173.
- Mitchell DM, Gennis RB (1995) Rapid Purification of Wildtype and Mutant Cytochrome c Oxidase from *Rhodobacter sphaeroides* by  $\text{Ni}^{2+}$ -NTA Affinity Chromatography. *FEBS Lett* 368: 148–150.
- Khailova LS, Prikhodko EA, Dedukhova VI, Mokhova EN, Popov VN, et al. (2006) Participation of ATP/ADP antiporter in oleate- and oleate hydroperoxide-induced uncoupling suppressed by GDP and carboxyatractylate. *Biochim Biophys Acta* 1757: 1324–1329.
- Samartsev VN, Mokhova EN, Skulachev VP (1997) The pH-dependent reciprocal changes in contributions of ADP/ATP antiporter and aspartate/glutamate antiporter to the fatty acid-induced uncoupling. *FEBS Lett* 412: 179–182.
- Palmer JW, Tandler B, Hoppel CL (1977) Biochemical properties of subsarcolemmal and interfibrillar mitochondria isolated from rat cardiac muscle. *J Biol Chem* 252: 8731–8739.
- Sugano T, Oshino N, Chance B (1974) Mitochondrial function under hypoxic conditions. The steady states of cytochrome c reduction and of energy metabolism. *Biochim Biophys Acta* 347: 340–358.
- Krab K, Wikstrom M (1987) Principles of coupling between electron transfer and proton translocation with special reference to proton-translocation mechanisms in cytochrome oxidase. *Biochim Biophys Acta* 895: 25–39.
- Krab K, Slater EC (1979) Ferrocyanide as electron donor to cytochrome  $a_3$ . Cytochrome c required for oxygen uptake. *Biochim Biophys Acta* 547: 58–69.
- Musatov AP, Berka V, Ksenzenko MY, Vygodina TV, Konstantinov AA (1991) Effect of Polycations on the Reaction of Cytochrome Oxidase with the Artificial Electron Donors and Cyanide. *Biological Membranes (Moscow)* 8: 229–234.
- Vygodina TV, Ptushenko VV, Konstantinov AA (2008)  $\text{Ca}^{2+}$  binding to cytochrome c oxidase affects redox properties of heme a. *Biochim Biophys Acta* 1777: S110–S111.
- Mills DA, Schmidt B, Hiser C, Westley E, Ferguson-Miller S (2002) Membrane Potential-controlled Inhibition of Cytochrome c Oxidase by Zinc. *J Biol Chem* 277: 14894–14901.
- Gellerich FN, Gizatullina Z, Nguyen HP, Trumbeckaite S, Vielhaber S, et al. (2008) Impaired regulation of brain mitochondria by extramitochondrial  $\text{Ca}^{2+}$  in transgenic Huntington disease rats. *J Biol Chem* 283: 30715–30724.
- Adiele RC, Stevens D, Kamunde C (2012) Differential inhibition of electron transport chain enzyme complexes by cadmium and calcium in isolated rainbow trout (*Oncorhynchus mykiss*) hepatic mitochondria. *Toxicol Sci* 127: 110–119.
- Vygodina TV, Dyuba AV, Konstantinov AA (2012) Effect of calcium ions on electron transfer between hemes a and  $a_3$  in cytochrome c oxidase. *Biochemistry (Moscow)* 77: 901–909.
- Kamiya K, Boero M, Tateno M, Shiraishi K, Oshiyama A (2007) Possible Mechanism of Proton Transfer through Peptide Groups in the H-Pathway of the Bovine Cytochrome c Oxidase. *J Am Chem Soc* 129: 9663–9673.
- Tsukahara T, Shimokata K, Katayama Y, Shimada H, Muramoto K, et al. (2003) The low-spin heme of cytochrome c oxidase as the driving element of the proton-pumping process. *Proc Natl Acad Sci USA* 100: 15304–15309.

## Acknowledgments

Thanks are due to Marten Wikstrom and Anne Puustinen (Helsinki Bioenergetics group) and to Bob Gennis (UIUC, IL) for kindly providing the bacterial mutant cytochrome oxidases D477A<sub>Pd</sub> and D485A<sub>Rs</sub>. We are much obliged to Artem Duba and Dr. N. Azarkina for discussion and help in preparation of the figures.

## Author Contributions

Conceived and designed the experiments: AAK TV. Performed the experiments: TV AK. Analyzed the data: AAK TV. Contributed reagents/materials/analysis tools: TV AK. Wrote the paper: AAK.

46. Yoshikawa S, Shinzawa-Itoh K, Tsukihara T (2000) X-ray structure and the reaction mechanism of bovine heart cytochrome *c* oxidase. *J Inorg Biochem* 82: 1–7.
47. Yoshikawa S (2003) A cytochrome *c* oxidase proton pumping mechanism that excludes the O<sub>2</sub> reduction site. *FEBS Lett* 555: 8–12.
48. Shimokata K, Katayama Y, Murayama H, Suematsu M, Tsukihara T, et al. (2007) The proton pumping pathway of bovine heart cytochrome *c* oxidase. *Proc Natl Acad Sci USA* 104: 4200–4205.
49. Yoshikawa S, Muramoto K, Shinzawa-Itoh K (2011) Proton-pumping mechanism of cytochrome *c* oxidase. *Annu Rev Biophys* 40: 205–223.
50. Egawa T, Yeh SR, Rousseau DL (2013) Redox-controlled proton gating in bovine cytochrome *c* oxidase. *PLoS One* 8: e63669.
51. Rich PR, Maréchal A (2013) Functions of the hydrophilic channels in protonmotive cytochrome *c* oxidase. *J R Soc Interface* 10: 20130183.
52. Starkov AA (1997) “Mild” uncoupling of mitochondria. *Biosci Rep* 17: 273–279.
53. Lee I, Bender E, Arnold S, Kadenbach B (2001) New control of mitochondrial membrane potential and ROS formation. *Biol Chem* 382: 1629–1636.
54. Yoshikawa S, Muramoto K, Shinzawa-Itoh K (2011) The O<sub>2</sub> reduction and proton pumping gate mechanism of bovine heart cytochrome *c* oxidase. *Biochim Biophys Acta* 1807: 1279–1286.
55. Kamiya K, Boero M, Tateno M, Shiraishi K, Oshiyama A (2007) First-principles molecular dynamics study of proton transfer mechanism in bovine cytochrome *c* oxidase. *J Phys Condens Matter* 19: 365220–365228.
56. Lee H-m, Das TK, Rousseau DL, Mills D, Fergusson-Miller S, et al. (2000) Mutations in the Putative H-Channel in the Cytochrome *c* Oxidase from *Rhodobacter sphaeroides* Show That This Channel Is Not Important for Proton Conduction but Reveals Modulation of the properties of Heme *a*. *Biochemistry* 39: 2989–2996.
57. Salje J, Ludwig B, Richter O-MH (2005) Is a third proton-conducting pathway operative in bacterial cytochrome *c* oxidase? *Biochem Soc Transactions* 33: 829–831.
58. Buschmann S, Warkentin E, Xie H, Langer JD, Ermler U, et al. (2010) The structure of *ccb<sub>3</sub>* cytochrome oxidase provides insights into proton pumping. *Science* 329: 327–330.
59. Ouyang H, Han H, Roh JH, Hemp J, Hosler JP, et al. (2012) The functional importance of a pair of conserved glutamic acid residues and of Ca<sup>2+</sup> binding in the *ccb<sub>3</sub>*-type oxygen reductases from *Rhodobacter sphaeroides* and *Vibrio cholerae*. *Biochemistry* 51: 7290–7296.
60. Ludwig B, Bender E, Arnold S, Huttemann M, Lee I, et al. (2001) Cytochrome *c* Oxidase and the Regulation of Oxidative Phosphorylation. *ChemBioChem* 2: 392–403.
61. Huttemann M, Lee I, Pecinova A, Pecina P, Przyklenk K, et al. (2008) Regulation of oxidative phosphorylation, the mitochondrial membrane potential, and their role in human disease. *J Bioenerg Biomembr* 40: 445–456.
62. Helling S, Huttemann M, Ramzan R, Kim SH, Lee I, et al. (2012) Multiple phosphorylations of cytochrome *c* oxidase and their functions. *Proteomics* 12: 950–959.
63. Capitanio N, Palese LL, Capitanio G, Martino PL, Richter OM, et al. (2012) Allosteric interactions and proton conducting pathways in proton pumping *aa<sub>3</sub>* oxidases: heme *a* as a key coupling element. *Biochim Biophys Acta* 1817: 558–566.
64. Kuznetsova SS, Azarkina NV, Vygodina TV, Siletsky SA, Konstantinov AA (2005) Zinc ions as cytochrome *c* oxidase inhibitors: two sites of action. *Biochemistry (Moscow)* 70: 128–136.
65. Lee HJ, Adelroth P (2013) The heme-copper oxidase superfamily shares a Zn<sup>2+</sup>-binding motif at the entrance to a proton pathway. *FEBS Lett* 587: 770–774.
66. Carafoli E (2010) The fateful encounter of mitochondria with calcium: How did it happen? *Biochim Biophys Acta* 1797: 595–606.
67. Naraghi M, Neher E (1997) Linearized Buffered Ca<sup>2+</sup> Diffusion in Microdomains and Its Implications for Calculation of [Ca<sup>2+</sup>] at the Mouth of a Calcium Channel. *J Neurosci* 17: 6961–6973.
68. Griffiths EJ, Balaska D, Cheng WHY (2010) The ups and downs of mitochondrial calcium signalling in the heart. *Biochim Biophys Acta* 1797: 856–864.
69. Spat A, Szanda G, Csordas G, Hajnoczky G (2008) High and low calcium-dependent mechanisms of mitochondrial calcium signalling. *Cell Calcium* 44: 51–63.
70. Balaban RS (2009) The role of Ca<sup>2+</sup> signaling in the coordination of mitochondrial ATP production with cardiac work. *Biochim Biophys Acta* 1787: 1384–1341.
71. Glancy B, Willis WT, Chess DJ, Balaban RS (2013) Effect of calcium on the oxidative phosphorylation cascade in skeletal muscle mitochondria. *Biochemistry* 52: 2793–2809.
72. Aon MA, Cortassa S, O'Rourke B (2010) Redox-optimized ROS balance: A unifying hypothesis. *Biochim Biophys Acta* 1797: 865–877.
73. Kirchok Y, Krapivinsky G, Clapham DE (2004) The mitochondrial calcium uniporter is a highly selective ion channel. *Nature* 427: 360–364.
74. Gunter TE, Pfeiffer DR (1990) Mechanisms by which mitochondria transport calcium. *Am J Physiol Cell Physiol* 258: C755–C786.
75. Rizzuto R, Marchi S, Bonora M, Aguilari P, Bononi A, et al. (2009) Ca<sup>2+</sup> transfer from ER to mitochondria: when, how and why. *Biochim Biophys Acta* 1787: 1342–1351.
76. Cheranov SY, Jagger JH (2004) Mitochondrial modulation of Ca<sup>2+</sup> sparks and transient K<sub>Ca</sub> currents in smooth muscle cells of rat cerebral arteries. *J Physiol* 556: 755–771.